

Identification of a novel potassium channel (GiK) as a potential drug target in *Giardia lamblia*: Computational descriptions of binding sites

Lisette Palomo-Ligas¹, Filiberto Gutiérrez-Gutiérrez²,
Verónica Yadira Ochoa-Maganda¹, Rafael Cortés-Zárate³,
Claudia Lisette Charles-Niño³ and Araceli Castillo-Romero³

¹ Departamento de Fisiología, Centro Universitario de Ciencias de la Salud, Universidad de Guadalajara, Guadalajara, Jalisco, Mexico

² Departamento de Química, Centro Universitario de Ciencias Exactas e Ingenierías, Universidad de Guadalajara, Guadalajara, Jalisco, Mexico

³ Departamento de Microbiología y Patología, Centro Universitario de Ciencias de la Salud, Universidad de Guadalajara, Guadalajara, Jalisco, Mexico

ABSTRACT

Background: The protozoan *Giardia lamblia* is the causal agent of giardiasis, one of the main diarrheal infections worldwide. Drug resistance to common anti-giardial agents and incidence of treatment failures have increased in recent years. Therefore, the search for new molecular targets for drugs against *Giardia* infection is essential. In protozoa, ionic channels have roles in their life cycle, growth, and stress response. Thus, they are promising targets for drug design. The strategy of ligand-protein docking has demonstrated a great potential in the discovery of new targets and structure-based drug design studies.

Methods: In this work, we identify and characterize a new potassium channel, GiK, in the genome of *Giardia lamblia*. Characterization was performed *in silico*. Because its crystallographic structure remains unresolved, homology modeling was used to construct the three-dimensional model for the pore domain of GiK. The docking virtual screening approach was employed to determine whether GiK is a good target for potassium channel blockers.

Results: The GiK sequence showed 24–50% identity and 50–90% positivity with 21 different types of potassium channels. The quality assessment and validation parameters indicated the reliability of the modeled structure of GiK. We identified 110 potassium channel blockers exhibiting high affinity toward GiK. A total of 39 of these drugs bind in three specific regions.

Discussion: The GiK pore signature sequence is related to the small conductance calcium-activated potassium channels (SKCa). The predicted binding of 110 potassium blockers to GiK makes this protein an attractive target for biological testing to evaluate its role in the life cycle of *Giardia lamblia* and potential candidate for the design of novel anti-giardial drugs.

Submitted 13 July 2018
Accepted 10 January 2019
Published 27 February 2019

Corresponding author
Araceli Castillo-Romero,
araceli.castillo@cucs.udg.mx

Academic editor
Mikko Karttunen

Additional Information and
Declarations can be found on
page 16

DOI 10.7717/peerj.6430

© Copyright
2019 Palomo-Ligas et al.

Distributed under
Creative Commons CC-BY 4.0

OPEN ACCESS

Subjects Bioinformatics, Computational Biology, Parasitology, Infectious Diseases, Computational Science

Keywords *Giardia lamblia*, Potassium channel, Potential target, Molecular modeling, Docking

INTRODUCTION

Giardia lamblia is the causal agent of giardiasis, a prolonged diarrheal disease. The standard compounds used against *Giardia lamblia* are 5-nitroimidazoles. However, these compounds present side effects associated with residual toxicity in the host. Dose-dependent side effects include leukopenia, headache, vertigo, nausea, insomnia, irritability, metallic taste, and CNS toxicity (Ansell *et al.*, 2015; Escobedo & Cimerman, 2007; Tejman-Yarden & Eckmann, 2011; Watkins & Eckmann, 2014). In addition, reports of resistant strains and nitroimidazole-refractory disease are of considerable concern. Reduced efficacy has been described even with higher drug doses (Carter *et al.*, 2018; Leitsch, 2015). For these reasons, there is a significant need for identification of new anti-*Giardia* drugs and drug targets. Ionic channels are pore-forming proteins that allow the passage of specific ions across the membrane, regulating different physiological processes (Subramanyam & Colecraft, 2015). Because of their biophysical behavior and participation in different human pathologies, ionic channels are attractive targets for drug design (Bagal *et al.*, 2013). Potassium channels are the most diverse and ubiquitous group of ion channels. They are divided into four main families on the basis of their biophysical and structural properties: voltage-gated K⁺ channels, calcium-activated K⁺ channels (K_{Ca}), inward-rectifier K⁺ channels and two-pore-domain K⁺ channels (K_{2P}) (Wulff, Castle & Pardo, 2009). In both electrically excitable and non-excitable cells, potassium channels regulate multiple cellular functions including cell volume, proliferation, differentiation, and motility (Grunnet *et al.*, 2002; Pchelintseva & Djamgoz, 2018; Schwab *et al.*, 2008; Urrego *et al.*, 2014).

Recently, several studies have reported identification and characterization of K⁺ channels in pathogenic protozoa. In *Plasmodium falciparum* and *Trypanosoma cruzi*, these channels are expressed in different stages of the parasite life cycle. They are essential for growth and play a significant role in parasite response to environmental stresses (Ellekvist *et al.*, 2004; Jimenez & Docampo, 2012; Waller *et al.*, 2008). A heterodimeric Ca²⁺-activated potassium channel was identified in *Trypanosoma brucei*. This identification was accomplished by profile searches of the predicted parasite proteome against the conserved loop of cation channels. The channel identified was found to be essential for the bloodstream form parasites (Steinmann *et al.*, 2015). The National Center for Advancing Translational Sciences Small Molecule Repository was screened. In this screening, fluticasone propionate was identified as a potential good inhibitor of *T. brucei* potassium channels. Experiments confirmed fluticasone propionate as a candidate drug targeting *T. brucei* (IC₅₀ of 0.6 μM) (Schmidt *et al.*, 2018). Biagini and coworkers showed that K⁺ causes an important depolarization of the membrane in *Giardia lamblia* (Biagini *et al.*, 2000). Results of others studies, report that K⁺ plays an important role as an osmolyte regulating *Giardia* cell volume (Maroulis, Schofield & Edwards, 2000). *Xenopus* oocytes were injected with mRNA isolated from trophozoites of *Giardia lamblia*, subsequent electrophysiology experiments revealed potassium currents (Ponce, Jimenez-Cardoso & Eligio-Garcia, 2013). By genome analysis and a bioinformatic approach, Prole and Marrion identified a putative potassium channel in

Giardia lamblia assemblage E (Prole & Marrion, 2012). However, the structural characterization of ionic channels in this protozoan is limited. Consequently, the potential of these channels to serve as a drug targets is poorly understood.

In recent years, *in silico* strategies have been used frequently to estimate protein function, for the discovery of new target molecules and for structure-based drug design studies (Chen & Chen, 2008). This work describes computational approaches to determine structural biology of a putative *Giardia* potassium channel, GiK. Further, this work evaluates the potential of this channel to serve as a novel target. A closed-state pore domain of GiK homology model was constructed. This construction was accomplished using a high conductance calcium-activated potassium channel from *Aplysia californica* (PDB ID: 5TJI) as a template. Our docking and virtual screening approach identified 110 potassium channel blockers exhibiting high free energy of binding to GiK, 39 of these drugs bind in the pore region of the channel. The drugs interact mainly with sites in three specific regions: S5, S2–S4 and C-terminal. These findings support the conclusion that this protein is an attractive target for biological testing to reveal its role in the life cycle of *Giardia lamblia* and a potential candidate for the design of novel anti-giardial drugs.

MATERIALS AND METHODS

In silico* putative potassium channel identification in *Giardia lamblia

To identify homologous sequences in *Giardia lamblia*, 51 potassium channel sequences from genomes of different species, deposited in the NCBI protein database (<http://www.ncbi.nlm.nih.gov/protein>), were compared by BLAST algorithm with the *Giardia* genome database (<http://giardiadb.org/giardiadb/>).

The amino acid composition, physicochemical properties, solvation and protein binding sites of the resulting sequence (GiK) (Accession number XP_001709490) were analyzed using PROTPARAM (<http://expasy.org/tools/>) and PredictProtein (Yachdav et al., 2014). We applied Predictor of Natural Disordered Regions (Obradovic et al., 2003) to predict disorder regions. Highly conserved residues were identified by consensus results of NCBI Conserved domains (Marchler-Bauer et al., 2017), Motif Search (<http://www.genome.jp/tools/motif/>), InterProScan tool (Jones et al., 2014), Block Searcher (Henikoff & Henikoff, 1994), and ExpASY PROSITE (Sigrist et al., 2013). Consensus results of the Constrained Consensus Topology prediction server (Tusnady & Simon, 1998, 2001) and PredictProtein (Yachdav et al., 2014) servers were used for the prediction of transmembrane domains.

Prediction of the potassium blockers binding sites on GiK

Homology model and refinement

The crystal structure of GiK is not available. Therefore, three-dimensional (3D) models of the pore region (1–500 aa) were produced using I-TASSER (Iterative Threading ASSEmbly Refinement) (Roy, Kucukural & Zhang, 2010; Yang et al., 2015; Zhang, 2008), RaptorX (Ma et al., 2012, 2013; Peng & Xu, 2010), Phyre2 (Protein Homology/analogy Recognition Engine V 2.0) (Kelley et al., 2015), SWISS-MODEL (Arnold et al., 2006; Biasini et al., 2014; Bordoli et al., 2008), and Modeller 9.18 (Fiser, Do & Sali, 2000;

Martí-Renom et al., 2000; Šali & Blundell, 1993; Webb & Sali, 2014). First, we searched the PDB (*Berman et al., 2007*) for known protein structures using the GiK sequence as query. We also searched for suitable templates in the SWISS-MODEL Template library. Next, a multiple alignment of the GiK sequence (UniProtKB accession: [A8B451](#)) to the main template structures was calculated, by MultAlin software (*Corpet, 1988*). Optimization of the hydrogen bonding network and the atomic level energy minimization of the 3D-GiK models generated were performed using the What If Web Interface (*Chinea et al., 1995*) and the 3D Refine protein structure refinement server (*Bhattacharya & Cheng, 2013; Bhattacharya et al., 2016*). The global structural quality of predicted models was validated by RAMPAGE (Ramachandran Plot Analysis) (*Lovell et al., 2003*), QMEAN (Qualitative Model Energy Analysis) (*Benkert, Tosatto & Schomburg, 2008*), Verify 3D (*Bowie, Luthy & Eisenberg, 1991; Luthy, Bowie & Eisenberg, 1992*), ERRAT (*Colovos & Yeates, 1993*) and ProSA-web (*Wiederstein & Sippl, 2007*). The 3D-GiK model with the best scoring was selected for refinement using UCSF CHIMERA v1.11.1 (*Pettersen et al., 2004*). We used 100 steps of conjugate gradient minimization. The QMEANBrane tool was used to assess the local quality of the 3D-GiK membrane protein model (*Studer, Biasini & Schwede, 2014*). To confirm the quality of the models, we compare the 13 resulting 3D models with the corresponding experimental structure using the root mean square deviation (RMSD). TM-align was used to determinate the backbone C α coordinates of the given protein structures. The results of the predicted models with C α -RMSD are expressed in Å. The monomer was built by alignment with template 5TJI. Tetrameric assemblage was obtained by the Maestro 2017-1 software with four holo forms monomers of 5TJIs, avoiding overlapping of monomers (Schrödinger, LLC, New York, NY, USA).

Molecular docking evaluation

Numerous structures of potassium blockers have been reported. To identify potential drug binding sites on the GiK protein, we selected 290 potassium blockers from the Drug bank (www.drugbank.ca), Sigma profile (www.sigmaldrich.com) and Zinc (<http://zinc.docking.org>) (*Irwin et al., 2012*) databases. Prior to docking, all structures were energy minimized using Maestro 2017-1 (Schrödinger, LLC, New York, NY, USA).

The docking simulations were carried out using AutoDock Vina software, employing a Lamarckian genetic algorithm (*Trott & Olson, 2010*), with a grid box of 126 Å³ and nine binding modes. The complexes and poses between 3D-GiK and potassium blockers were analyzed using Maestro 2017-1 (Schrödinger, LLC, New York, NY, USA). The results are reported as binding energy of ligand and protein in kcal/mol.

RESULTS

Identification and characterization of the putative potassium channel GiK

We performed BLAST searches of the *Giardia* genome database. We used the whole sequence of 51 potassium channels genomic sequences of different species as queries ([Table S1](#)).

The uncharacterized protein GL50803_101194, GiK (GenBank Accession: [XP_001709490](#)),

Table 1 Sequences producing significant alignments with GiK by BLAST.

Accession number	Organism	Type of channel	Score	E. value	Identities	Positives
BAN90095.1	<i>Aeropyrum camini</i>	Kv	32	0.33	15/49 (31%)	29/49 (59%)
AEE68730.1	<i>Bordetella pertussis</i>	Kv	32	0.51	15/43 (35%)	25/43 (58%)
WP_012338231.1	<i>Burkholderia cenocepacia</i>	Kv	33	0.20	16/39 (41%)	25/39 (64%)
YP_002407586.1	<i>Escherichia coli</i>	Kv	28.9	8.6	18/66 (27%)	36/66 (55%)
WP_024212520.1	<i>Escherichia spp</i>	Multispecies Kv	28.9	9.8	18/66 (27%)	36/66 (55%)
AAP94028.1	<i>Gallus gallus</i>	Kv1.3	34.7	0.27	20/58 (34%)	32/58 (55%)
WP_011570442.1	<i>Haloquadratum walsby</i>	Ion channel	33	0.18	10/20 (50%)	18/20 (90%)
AAA61276.1	<i>Homo sapiens</i>	Kv	35	0.24	16/43 (37%)	25/43 (58%)
NP_002223.3	<i>Homo sapiens</i>	Kv1.3	35.0	0.17	20/58 (34%)	32/58 (55%)
CDS30290.2	<i>Hymenolepis microstoma</i>	Kv	32.7	2.4	22/80 (28%)	40/80 (50%)
AEO96823.2	<i>Lateolabrax japonicus</i>	Kv1.3	33.1	0.56	18/45 (40%)	26/45 (58%)
CCQ21618.1	<i>Listeria monocytogenes</i>	Kv	36	0.012	14/41 (34%)	27/41 (66%)
NP_001245037.1	<i>Macaca mulatta</i>	Kv1.3	35.0	0.18	20/58 (34%)	32/58 (55%)
NP_032444.2	<i>Mus musculus</i>	Kv1.3	33.5	0.47	14/38 (37%)	24/38 (63%)
XP_007383667.1	<i>Punctularia strigosozonata</i>	Kv	44	5e-04	33/105 (31%)	53/105 (50%)
WP_006887331.1	<i>Rothia aeria</i>	Kv	36.6	0.032	17/67 (25%)	34/67 (51%)
NP_707157.2	<i>Shigella flexneri 2a str. 301</i>	Kv	29	5.3	18/66 (27%)	36/66 (55%)
CAA56175.1	<i>Solanum tuberosum</i>	Kir	32.0	1.9	18/67 (27%)	34/67 (51%)
NP_631700.1	<i>Streptomyces coelicolor</i>	Kv	30	0.54	9/34 (26%)	24/34 (71%)
CDW52461.1	<i>Trichuris trichiura</i>	Kv	31.6	1.9	12/49 (24%)	27/49 (55%)
AUI87359.1	<i>Vibrio azureus</i>	Kv	31.6	1.3	27/91 (30%)	46/91 (51%)

Table 2 Physicochemical characterization of GiK by Protparam.

Number of amino acids	1,416
Molecular weight	25,811.2
Instability index	45.47
Aliphatic index	93.28
Grand average of hydropathicity (Gravy)	-0.053
Isoelectric point	8.18
Ext. Coeficiente	141,880

showed 24–50% identity and 50–90% positivity with 21 different types of voltage-gated potassium channels (Table 1). Physicochemical properties were obtained (Table 2).

These properties enabled establishment of GiK molecular weight, stability index, isoelectric point, aliphatic index, and Grand Average of Hydropathicity (GRAVY) of GiK.

The instability index indicates that GiK might be unstable in nature (instability index > 40). The aliphatic index, a factor in protein thermal stability, is related to the mole fraction of Ala, Ile, Leu, and Val in the protein. The aliphatic index of GiK 93.28 indicates a thermally stable protein that contains high amount of hydrophobic amino acids (Fig. S1). The negative value of GRAVY indicates that GiK is a hydrophilic protein (Wilkins et al., 1999).

The prediction of disordered regions in GiK suggests that this protein has 11 intrinsically

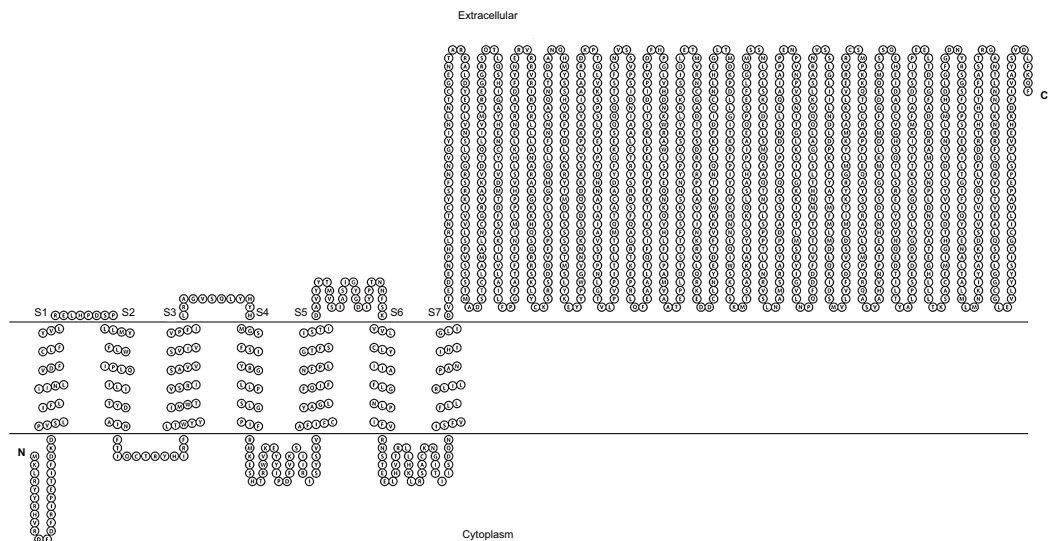


Figure 1 Transmembrane structure of GiK. It contains seven transmembrane segments (S1–S7), the P-loops between S5 and S6 form the pore domain. The selectivity filter is in gray.

Full-size DOI: [10.7717/peerj.6430/fig-1](https://doi.org/10.7717/peerj.6430/fig-1)

disordered regions (IDRs) that could be involved in important *Giardia* functions (Fig. S2). The membrane topology and the analysis of the main features of K^+ channels show that GiK is a membrane protein that possesses seven helical transmembrane (HTM) regions. Further, evidence shows a highly conserved pore-loop sequence that determines K^+ channel selectivity (Fig. 1). According to databases of protein signatures, GiK contains: a domain related to ionic channels, Ion_trans_2 domain; domains related to voltage-gated potassium channels, 215625 and 236711; one domain associated with signal transduction, 227696; two fingerprints of potassium channel, 2POREKCHANNEL and KCHANNEL; and one fingerprint related with EAG/ELK/ERG channels (EAGCHANLFMLY). These results suggest that this protein is a potassium channel (Fig. 2; Table 3).

The pore-forming domain is highly conserved in all types of K^+ channels. An alignment revealed that all sequences that showed homology with GiK present the pore signature sequence S/TXGXGX. GiK has the residues SIASIGYGD, similar to TFLSIGYG, which are present in small conductance calcium-activated potassium channels (SKCa) (Shin *et al.*, 2005) (Fig. 3). Finally, using PredictProtein server (Yachdav *et al.*, 2014), we predicted GiK has potassium channel activity with 36% reliability.

Modeling and structure quality of GiK protein

The prediction of the 3D-GiK structure was done by homology modeling. The search for a structural template for GiK protein revealed identity with four resolved protein structures. Two structures were the open and closed state of a high conductance calcium-activated potassium channel from *A. californica* (PDB ID: 5TJ6, open state, and 5TJI, closed state), with 23% sequence identity. The other two structures were the open and closed state of a potassium channel subfamily T member one from *Gallus gallus* (PDB: 5U70, open state, and 5U76, closed state) with 19% sequence identity (Fig. S3).

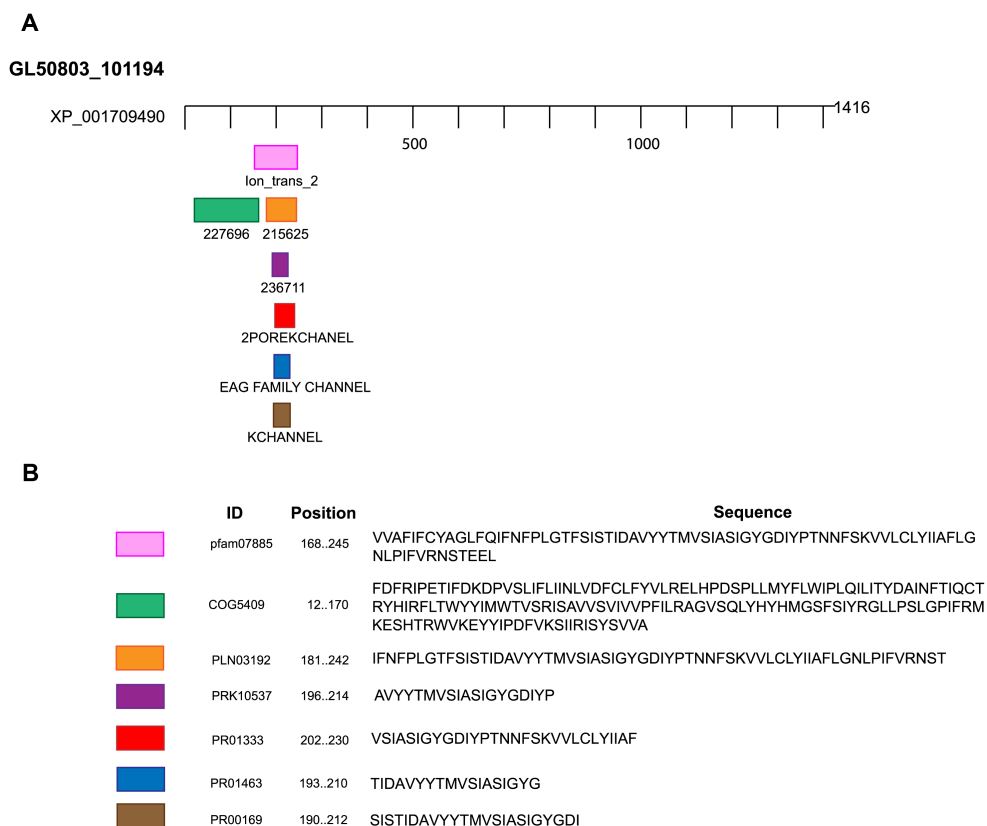


Figure 2 Domains and motifs related to potassium channels. GiK presents domains related to different subtypes of potassium channels. (A) Schematic representation. (B) Accession number and description of the sequences. [Full-size !\[\]\(fd7fe780e8fd8eece60268c87d0c3e04_img.jpg\) DOI: 10.7717/peerj.6430/fig-2](https://doi.org/10.7717/peerj.6430/fig-2)

Table 3 Prediction of highly conserved residues from GiK.

Domain or motif	Description	Accession number	Position (<i>E</i> value)	Server
Ion_trans_2	Ionic channel. This family includes the two membrane helix type ion channels found in bacteria.	pfam07885	168–245 (1.35e-08)	NCBI Conserved domains, Motif search, InterProScan tool
227696	EXS domain-containing protein (Signal transduction mechanisms).	COG5409	12–170 (0.44)	ExPASy PROSITE, Motif search
215625	Voltage-dependent potassium channel; Provisional.	PLN03192	181–242 (0.14)	ExPASy PROSITE, Motif search
236711	Voltage-gated potassium channel; Provisional.	PRK10537	196–214 (0.70)	ExPASy PROSITE, Motif search
2POREKCHANNEL	Potassium channel domain.	PR01333	202–230 (0.00032)	Block searcher
EAGCHANLFMLY	EAG/ELK/ERG potassium channel family signature.	PR01463	193–210 (0.029)	Block searcher
KCHANNEL	Potassium channel signature.	PR00169	190–212 (0.1)	Block searcher

Model construction was performed using five homology modeling servers: I-TASSER, RaptorX, Phyre2, Swiss model, and Modeller 9.18. Using the four templates, a modeling protocol was constructed for each program. The final dataset includes

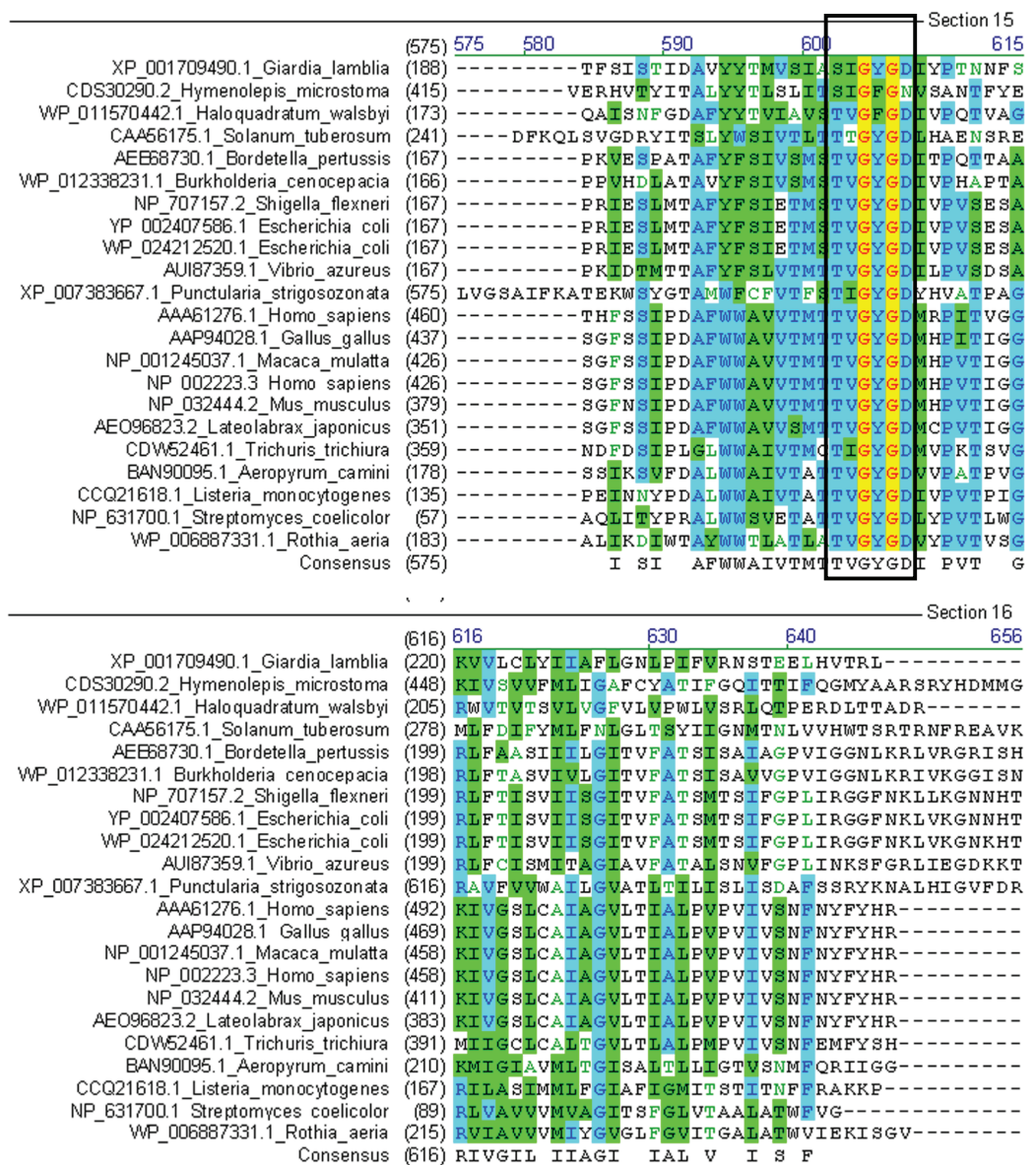


Figure 3 Multiple sequence alignment of GiK with voltage-gated potassium channels. The signature sequence T/SXGXG of the selectivity filter is present in all classes of potassium channels (black square).

Full-size  DOI: 10.7717/peerj.6430/fig-3

13 3D-GiK models covering a wide range of quality. The global quality of each theoretical model was validated by the Ramachandran plot analysis, QMEAN score, Z score, ERRATscore, and Verify 3D. Modeller 9.18 program produced the best 3D-GiK model, using the sequence 5TJI as template (Table 4). Figures 4A–4C show the resulting ratio of Z-score and the QMEAN score obtained for GiK. The z-score value, -5.07 , is in the range of native conformations. This can be seen clearly when the score is compared to the scores of other experimentally determined protein structures with the same number of residues. Further, the QMEAN4 score is in the range of a good experimental structure (0.296). Additionally, the Ramachandran plot analysis confirms that this model is

Table 4 Validation scores from RAMPAGE, QMEAN, ProSA-web, ERRAT, and Verify 3D of the constructed models.

Software	Template (PDB ID)	Ramachandran (%)	QMEAN score	Z-score	ERRAT score	Verify 3D	Residues	RMSD (Å)
Modeller	5TJ6	90.4	0.141	-7.56	44.26	26.28	500	4.28
	5U70	90.0	0.094	-8.09	39.62	14.06	500	5.05
	5TJI	94.2	0.296	-5.07	69.24	35.60	500	3.90
	5U76	88.4	0.023	-9.22	34.97	26.28	500	4.46
Raptorx	5TJ6	89.8	0.191	-6.92	56.64	20.60	500	4.85
I-tasser	5TJ6	72.9	0.101	-8.78	86.58	38.80	500	3.97
	5U70	69.6	0.089	-9.12	81.91	44.60	500	5.01
Swiss model	5TJ6	89.8	0.205	-6.21	81.48	33.00	296	0.92
	5U70	92.8	0.271	-5.53	87.54	39.38	292	0.91
	5TJI	92.5	0.240	-5.82	88.57	30.98	296	1.12
	5U76	92.9	0.191	-6.34	84.17	26.35	297	1.17
Phyre2	5TJ6	95.7	0.239	-5.72	61.63	37.36	265	1.01
	5U76	94.7	0.251	-5.99	35.04	38.44	372	1.10

characterized by stereochemical parameters of a stable structure, with 94.2% of residues in the most favored region, 4.6% in the allowed region, and 1.2% in the disallowed region (Fig. 4). Finally, according to the QMEANBrane tool estimation, the 3D-GiK model is in the range expected for a membrane protein (Fig. 5). Figure 6 shows the monomeric and tetrameric form, and the pore cavity.

Molecular docking

Molecular docking permits prediction of the most probable position, orientation, and conformation of interactions between a ligand and macromolecule (Ferreira et al., 2015). To predict binding free energy to GiK, 290 potassium blockers were investigated (Table S2). The overall docking energy of a given ligand molecule was expressed in kcal/mol. This approach revealed 110 molecules exhibiting the best binding free energies (-4 to -11 kcal/mol) (Table 5). Of these, 39 are commercially available compounds. Interestingly, these drugs bind in three specific hydrophobic pockets of GiK. We labeled these regions I, II, and III (Fig. 7). As shown in Table 6, 13 residues are important for binding in region I, located on the S6 transmembrane region of the channel. Of these, 10 are hydrophobic and three are polar. For region II, nine residues located on the S5-S6 linker and S6 portion of the channel interact with the various docked ligands. Of these, five are hydrophobic and four are polar. For region III, 12 extracellular residues are important for ligand interaction. Eight are hydrophobic and four are polar. The major residues observed to interact with more of the ligands were Leu65, Gly113, Gln116, Leu117, Tyr120, Met122, Phe125, Ile127, and Arg129, in region II. More negative free binding energy results in the formation of stronger complexes. We analyzed the interaction maps of the three molecules with highest binding free energies that bind to different pockets of the GiK protein. The ligand with the highest score was the K⁺ channel blocker 6,10-diaza-3(1,3)8,(1,4)-dibenzena-1,5(1,4)-diquinolincy clodecaphane

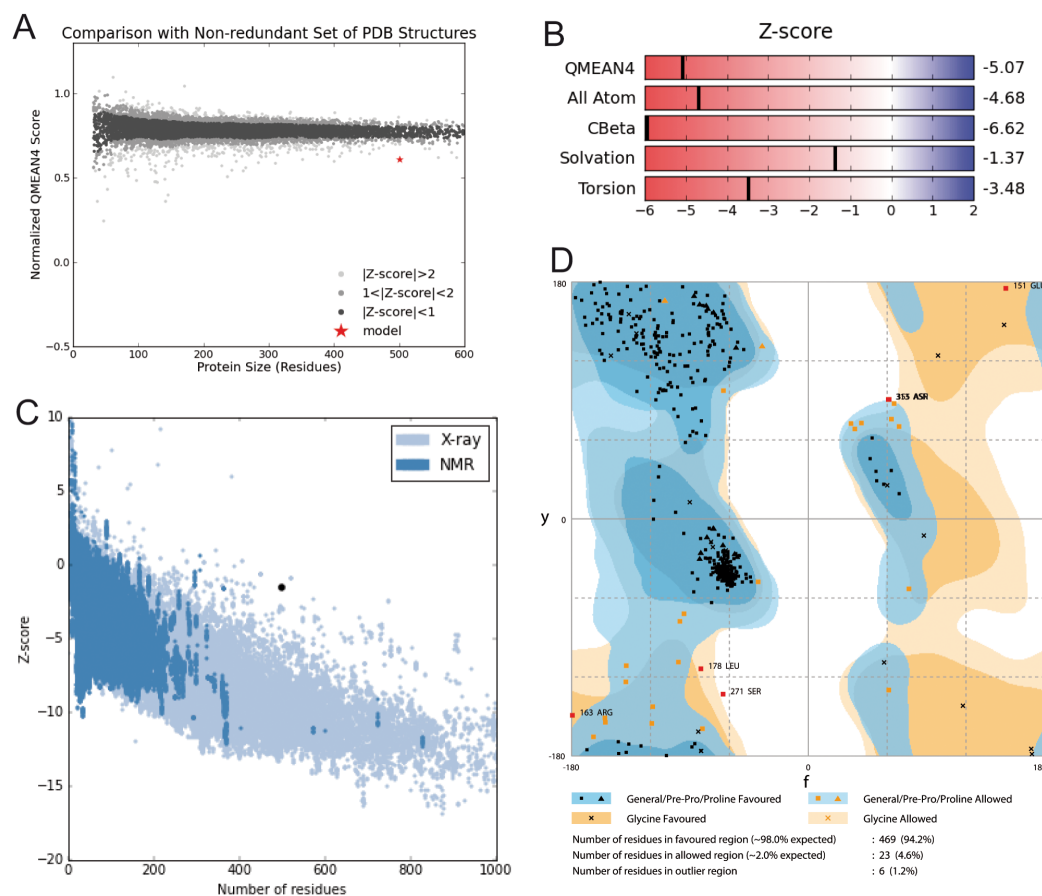


Figure 4 Structural validation. (A) Normalized QMEAN score of theoretical 3D structure for GiK protein model created with SWISS-MODEL server. (B) Graphical representation of the Z-Score of the individual component of QMEAN. (C) ProSA-web Z-scores of all proteins chains in PDB determined by X-ray crystallography (light blue) or NMR spectroscopy (dark blue). The Z score of GiK is highlighted as a black dot. (D) Ramachandran plot analysis, 94.2% of total residues are in the most favored region.

Full-size DOI: 10.7717/peerj.6430/fig-4

(UCL 1684, -11.2 kcal/mol). This drug was observed to interact with GiK in region I forming hydrophobic interactions with Phe218, Val221, Val222, Leu225, Tyr226, Val247, Leu250, and Leu276. The competitive antagonist of GABA_A receptors, bicuculline, had the highest score (-10 kcal/mol) for interaction with GiK in region II. This drug forms: hydrophobic interactions with Gly113, Gln116, Leu117, Tyr118, Tyr120, Met122, Ser124, Phe125, Ser126, and Arg129. Further, bicuculline forms π - π interactions with Phe125 and Tyr68. Finally, the bioactive alkaloid, verruculogen, interacts with GiK site III by hydrophobic interactions with Val348, Pro347, Val377, Met378, and Ile411. Further, verruculogen interacts by polar interaction with Ser346 (Table 6; Fig. 8).

DISCUSSION

In this report, we provide *in silico* evidence indicating the protein XP_001709490 from *Giardia lamblia* (GiK) is a membrane protein, with conserved potassium channels features. GiK presents seven HTM regions and the pore signature sequence SIASIGYGD.

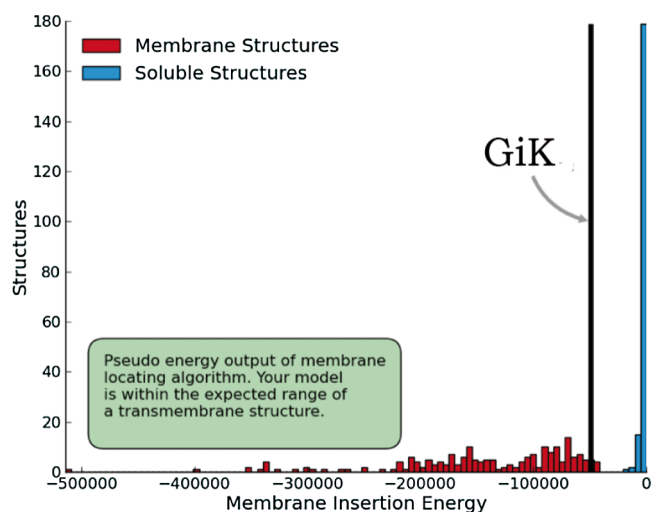


Figure 5 Quality estimation of GiK as a membrane protein. Prediction done with SWISS-MODEL-QMEANBrane tool. [Full-size !\[\]\(ba1b80118482ccef74a5d718ca4d7242_img.jpg\) DOI: 10.7717/peerj.6430/fig-5](https://doi.org/10.7717/peerj.6430/fig-5)

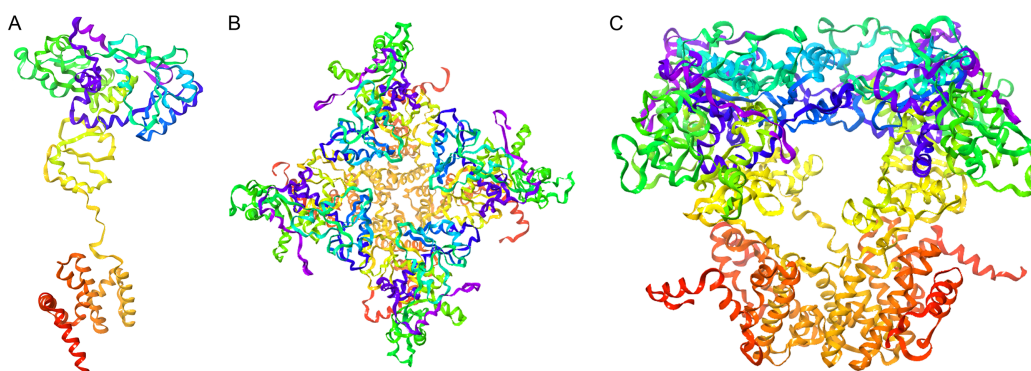


Figure 6 Representation of the 3D-GiK modeled structure. (A) Monomer, (B and C) Tetramer. The images were generated using Maestro software. [Full-size !\[\]\(ab8f7a9d25e63edc6ae9f62ddaa1d31c_img.jpg\) DOI: 10.7717/peerj.6430/fig-6](https://doi.org/10.7717/peerj.6430/fig-6)

This sequence is associated with K^+ selectivity in SKCa. The presence of the Ion_trans_2 domain related to voltage-gated potassium channels suggests that GiK could be activated by either electrical means or by increasing calcium concentrations in the cell. Additional studies are necessary to understand the voltage-gated and ion selectivity in GiK.

Transmembrane protein GiK presents hydrophobic regions containing a high fraction of non-polar amino acids. It also presents hydrophilic regions containing a high fraction of polar amino acids (Figs. S1 and S4). The GRAVY value of -0.053 indicates that GiK could establish interactions with water; it can be highly hydrated in aqueous media. GiK contains protein regions that do not fold into defined tertiary structure. These are structural disorders commonly labeled IDRs. IDRs perform a central role in regulation of signaling pathways and crucial cellular processes. They are frequently associated with disease. For these reasons, there is growing interest in IDRs as potential targets for drug design (Calcada, Korsak & Kozyreva, 2015; Cheng et al., 2006).

Table 5 Best docking score values (kcal/mol) from the potassium channel blockers to 3D-GiK model.

Compound	Docking score (kcal/mol)	Compound	Docking score (kcal/mol)	Compound	Docking score (kcal/mol)
UCL_1684	-11.2	ZINC13489790	-8	Flecainide	-6.9
ZINC38144725	-10.8	Imipramine	-7.9	Mepivacaine	-6.9
Terfenadine	-10.6	Trifluoroperazine	-7.9	ZINC13489786	-6.8
ZINC00018512	-10.4	ZINC13489791	-7.9	ZINC13760202	-6.8
ZINC00598948	-10.1	ZINC13489800	-7.9	ZINC13777065	-6.8
Bicuculine	-10	ZINC13489804	-7.9	1-Ethyl-2-Benzimidazolinone	-6.7
Cromoglicic acid	-10	ZINC13489830	-7.9	ZINC13760207	-6.7
Penitrem_A	-10	ZINC13760212	-7.9	ZINC13760214	-6.7
BMS_204352	-9.4	Linopirdine	-7.8	ZINC03935230	-6.5
NS1643	-9.1	ZINC13442157	-7.8	ZINC13557606	-6.5
Paxilline	-9.1	ZINC13489810	-7.8	ZINC13777062	-6.5
CP_339818	-9	ZINC13489818	-7.8	ZINC27617403	-6.5
Tubocurarine	-8.9	ZINC13489829	-7.8	Dofetilide	-6.4
ZINC13489797	-8.8	ZINC13489785	-7.7	Retigabine	-6.4
UK_78282	-8.7	TRAM_34	-7.6	ZINC00005768	-6.4
Verruculogen	-8.7	ZINC13489794	-7.6	ZINC13760203	-6.4
ZINC13489806	-8.6	ZINC13489798	-7.6	ZINC13777063	-6.4
ZINC13644028	-8.6	ZINC13489784	-7.5	ZINC13777067	-6.4
DIDS	-8.5	ZINC13489803	-7.5	Correolide	-6.3
ZINC01535217	-8.5	ZINC13489813	-7.5	ZINC03935234	-6.3
ZINC13442159	-8.5	ZINC13557604	-7.5	ZINC03935235	-6.3
ZINC38144724	-8.5	Amitriptyline	-7.4	ZINC03946466	-6.3
Bicuculine methiodide	-8.4	Dequalinium	-7.4	ZINC13777069	-6.3
ZINC13489814	-8.4	ZINC01539875	-7.4	ZINC13777072	-6.3
ZINC13489817	-8.4	ZINC13489789	-7.4	Procaine	-6.2
ZINC00015850	-8.3	Quinidine	-7.3	Zoxazolamine	-6.1
ZINC00603820	-8.3	ZINC00014006	-7.3	ZINC13777058	-6
ZINC01539867	-8.2	ZINC01535218	-7.3	ZINC18096411	-6
ZINC13489795	-8.2	ZINC13760206	-7.3	ZINC13777075	-5.8
ZINC13489796	-8.2	ZINC27617400	-7.3	ZINC13643922	-5.7
ZINC13489807	-8.2	Psora_4	-7.2	Chlorzoxazone	-5.5
ZINC13489823	-8.2	ZINC18189761	-7.2	ZINC13579814	-5.5
ZINC29309163	-8.2	Pimaric_acid	-7.1	LY_97241	-5
Niguldipine	-8.1	Miconazole	-7	Clofilium	-4.8
ZINC13489799	-8.1	ZINC13760204	-7	Halothane	-4.5
XE991	-8	ZINC13760205	-7	4_Aminopyridine	-4.4
ZINC01539870	-8	ZINC13760213	-7		

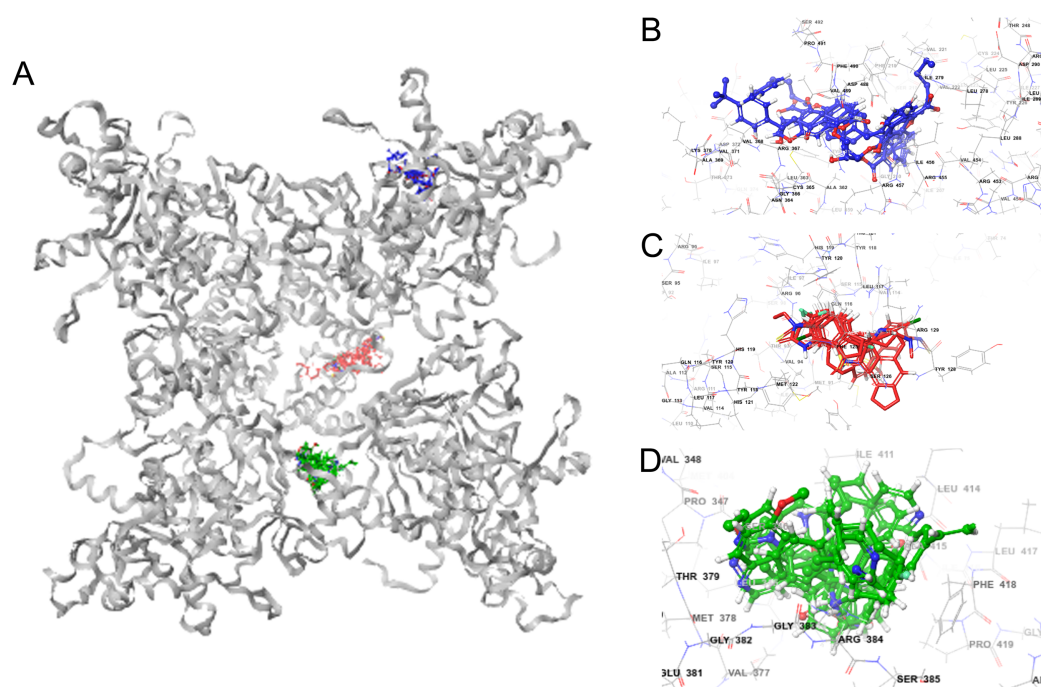


Figure 7 GiK—potassium channel blockers docking simulations (A); (B–D) magnified views of the boxed regions depict the three potassium blockers channels binding sites (blue region I, red region II and green region III). [Full-size](#) DOI: 10.7717/peerj.6430/fig-7

Table 6 Binding sites from the potassium channel blockers to GiK.

Region	Amino acid residues	Potassium channel blockers
I	Phe218, Val221, Val222, Leu225, Tyr226, Leu250, Leu278, Ile279, Ile456, Arg457, Asp488, Val489, Phe490	UCL_1684, terfenadine, cromoglicic acid, CP_339818, niguldipine, imipramine, Psora_4, mepivacaine, procaine, chlorzoxazone, 4_Aminopyridine
II	Leu65, Gly113, Gln116, Leu117, Tyr120, Met122, Phe125, Ile127, Arg129	Bicuculine, Penitrem_A, BMS_204352, NS1643, paxilline, tubocurarine, UK_78282, DIDS, bicuculine methiodide, trifluoroperazine, amitriptyline, dequalinium, miconazole, flecainide, 1-Ethyl-2-Benzimidazolinone, correolide, clofilium, halothane
III	Val344, Leu345, Ser346, Val377, Thr379, Gly383, Arg384, Leu388, Leu414, Ala415, Phe418, Pro419	Verruculogen, XE991, linopirdine, TRAM_34, quinidine, pimaric_acid, dofetilide, retigabine, zoxazolamine, LY_97241

The prediction of 14 flexible disordered regions in GiK suggests that this protein may be important in various *Giardia* functions. This important preliminary evidence indicates that GiK is a promising subject for future study.

Potassium channels regulate multiple cellular functions in both electrically excitable and non-excitable cells. Therefore, they are attractive targets for drug design.

Current trends in drug discovery focus on target identification and *in silico* compound

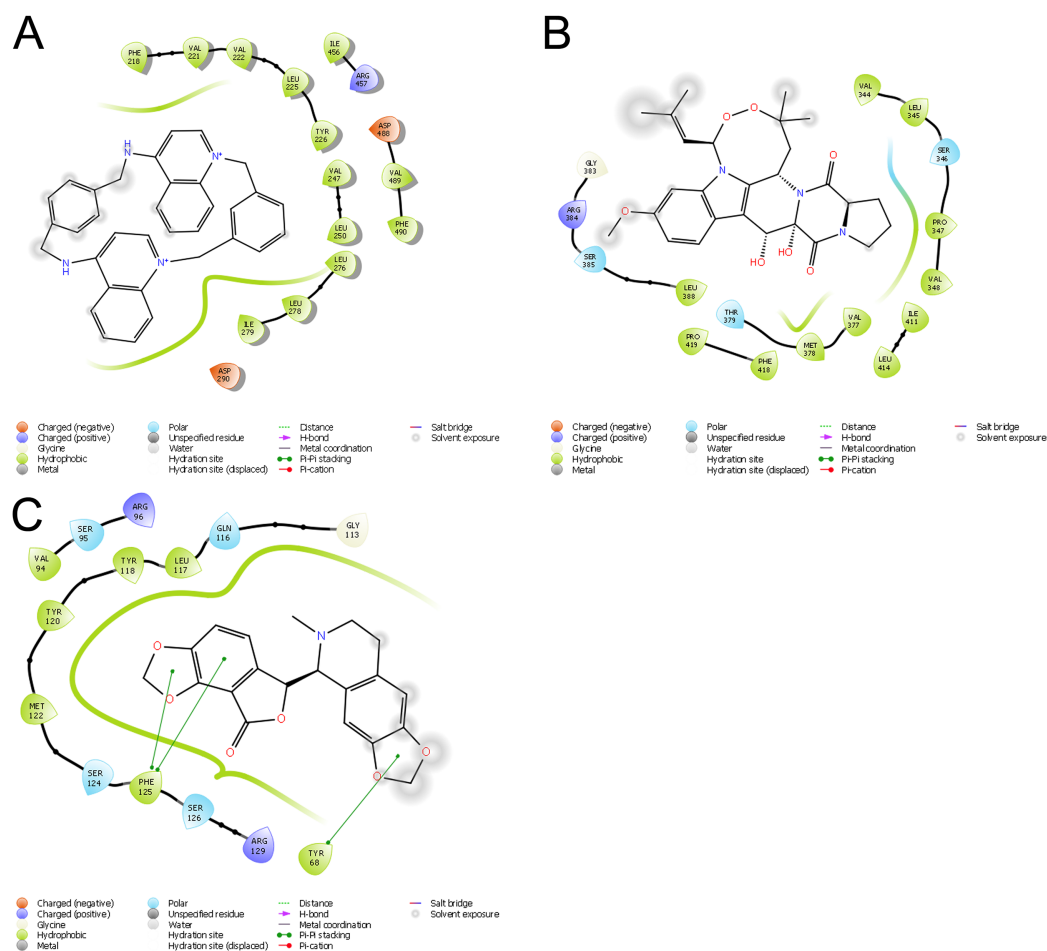


Figure 8 Ligand interaction diagrams. UCL 1684 (A), Bicuculline (B) or verruculogen (C). Hydrophobic interactions are depicted by green curves, π - π interactions are in green-dashed lines, and the polar interactions by curve blue lines. [Full-size](#) DOI: 10.7717/peerj.6430/fig-8

design. We sought to determine whether GiK could be a potential drug target in *Giardia*. First, we built structural models of the transmembrane helical regions of GiK by homology modeling. The search for templates showed only two resolved structures: a high conductance calcium-activated potassium channel from *A. californica* (PDB ID: 5TJ6 and 5TJI) and a potassium channel subfamily T member one from *Gallus gallus* (PDB: 5U70 and 5U76). In this work, GiK presents 23% and 19% of sequence identity with the templates. RMSD is a quantitative measure of the similarity between two superimposed atomic coordinates. When using RMSD to compare protein structures, the RMSD distribution depends on the size of the protein and of the homology between the templates, among others (*Kufareva & Abagyan, 2012*). Using multiple approaches we generated 13 structural models of GiK, the quality analysis of individual models showed that even though, models obtained with Swiss model and Phyre2 had the lower RMSD values, only 50–70% of residues were modeled. The percentage of residues in the allowed regions was expected to be more than 90% for a good model. The Modeller program produced acceptable models. The best result was obtained employing the PDB ID:

5TJI (closed state); 500 aa aligned, results from a Ramachandran plot showed 94.2% of residues in the most favored region. Even though the structures obtained with 5U70 and 5TJ6 showed 90% of residues in the most favored region, the overall quality factor (Bagal *et al.*, 2013) value of 5TJI is the highest (69.24%) and is within the accepted range. Besides, it is important to emphasize that in addition to RMSD, the generation of Z-score is also a measure of statistical significance between matched structures and reflects the degree of modeling success (Dalton & Jackson, 2007), the Z-score value (−5.07) indicates that the overall geometrical quality of the model generated by Modeller using the template 5TJI was within the acceptable range for big proteins. The overall results from RAMPAGE, QMEAN and Verify 3D indicate the 3D modeled GiK protein is of good quality. After building the 3D structure of GiK, we screened 290 potassium channel blockers. The docking results showed 110 potassium channel blockers with high affinity for the GiK protein. A total of 39 of these showed similar binding modes in three specific regions, labelled I to III. They interact principally with hydrophobic and aromatic residues such as Phe, Tyr, Leu, and Val. In agreement with results described for different potassium blockers, the ring stacking, hydrophobic interactions with several aromatic side chains and polar interactions take place mainly in S5 and S6 (Marzian *et al.*, 2013; Saxena *et al.*, 2016). The ionic channels can be switched or gated between an open and closed state by external signals such as changes in transmembrane voltage, binding of ligands, and mechanical stress. Some K⁺ channels possess a highly hydrophobic inner pore that can function as an effective barrier to ion permeation (Aryal, Sansom & Tucker, 2015). Our results suggest that GiK is a calcium potassium activated channel with a hydrophobic inner pore. Additional research is needed to confirm this finding. We plan to expand our studies in this area in the future (Liu & Kokubo, 2017; Martins *et al.*, 2018).

Other authors have reported successful computational screening of K⁺ channels. These reports demonstrate that computational screening is an effective method for rapidly discovering new channels blockers from large databases (Kingsley *et al.*, 2017; Liu *et al.*, 2003). Hong Liu and coworkers identified 14 natural compound of relatively lower binding energy. These researchers used a docking virtual screening approach based upon a 3D model of the eukaryotic K⁺ channels. Experimental results showed that four of these exerted potent and selective inhibitory effect on K⁺ channels (Liu *et al.*, 2003). Interestingly, some of the potassium channel blockers in our study have been employed with some success for their antiparasite activity. Verruculogen, clofilium, clotrimazole, trifluoroperazine, bicuculline methiodide, tubocurarin, and dequalinium chloride affect the growth of *Trypanosoma brucei*, *Leishmania donovani*, *Plasmodium falciparum*, and *Trichomonas vaginalis* (Della Casa *et al.*, 2002; Nam *et al.*, 2011; Rateb *et al.*, 2013; Waller *et al.*, 2008). Quinidine inhibits the cell division in *Tetrahymena pyriformis* (Conklin, Heu & Chou, 1970). Trifluoroperazine alters the motility in *Paramecium sp.* (Otter, Satir & Satir, 1984). Disodium cromoglycate and terfenadine show activity in infection models of *Toxoplasma gondii* and *Plasmodium yoelli nigeriensis* (Rezaei *et al.*, 2016; Singh & Puri, 1998). In *Giardia lamblia*, trifluoroperazine, a calmodulin

antagonist, inhibits excystment (*Bernal et al., 1998*). It remains uncertain whether potassium channels are the targets of these compounds.

CONCLUSION

Using structural bioinformatics, we identified the hypothetical protein [XP_001709490](#) from *Giardia lamblia* as a potassium channel, GiK. By protein docking analysis, we found 39 commercial potassium channel blockers that have affinity for this protein. These blockers are predicted to bind in three specific regions on the protein. The novelty of this work lies in the use of the model 3D-GiK structure to screen compounds with theoretical affinity. Some of the drugs predicted by the model to be effective have demonstrated antiparasitic activity in *in vitro* and *in vivo* assays. Experimental analyses are needed to confirm the activity of these drugs on *Giardia*. The low homology of GiK with proteins in the human genome contributes to its potential as a target of specific pharmacological agents.

ADDITIONAL INFORMATION AND DECLARATIONS

Funding

Lissethe Palomo, Filiberto Gutiérrez and Verónica Ochoa awarded scholarships 377019, 574252 and 575532 from CONACYT. This work was partially supported by the Fondo Sectorial de Investigación en Salud y Seguridad Social (CONACYT-FOSISS 2015-1-261442). There was no additional external funding received for this study. The funders had no role in study design, data collection and analysis, decision to publish, or preparation of the manuscript.

Grant Disclosures

The following grant information was disclosed by the authors:

Lissethe Palomo, Filiberto Gutiérrez and Verónica Ochoa awarded scholarships: 377019, 574252 and 575532 from CONACYT.

Fondo Sectorial de Investigación en Salud y Seguridad Social: CONACYT-FOSISS 2015-1-261442.

Competing Interests

The authors declare that they have no competing interests.

Author Contributions

- Lissethe Palomo-Ligas conceived and designed the experiments, performed the experiments, analyzed the data, prepared figures and/or tables, authored or reviewed drafts of the paper, approved the final draft.
- Filiberto Gutiérrez-Gutiérrez conceived and designed the experiments, performed the experiments, analyzed the data, contributed reagents/materials/analysis tools, prepared figures and/or tables, authored or reviewed drafts of the paper, approved the final draft.
- Verónica Yadira Ochoa-Maganda performed the experiments, analyzed the data, authored or reviewed drafts of the paper, approved the final draft.

- Rafael Cortés-Zárate contributed reagents/materials/analysis tools, authored or reviewed drafts of the paper, approved the final draft.
- Claudia Lisette Charles-Niño contributed reagents/materials/analysis tools, authored or reviewed drafts of the paper, approved the final draft.
- Araceli Castillo-Romero conceived and designed the experiments, analyzed the data, contributed reagents/materials/analysis tools, prepared figures and/or tables, authored or reviewed drafts of the paper, approved the final draft.

Data Availability

The following information was supplied regarding data availability:

Raw data are available in the [Supplemental Files](#).

Supplemental Information

Supplemental information for this article can be found online at <http://dx.doi.org/10.7717/peerj.6430#supplemental-information>.

REFERENCES

- Ansell BRE, McConville MJ, Ma'ayeh SY, Dagley MJ, Gasser RB, Svard SG, Jex AR. 2015.** Drug resistance in *Giardia duodenalis*. *Biotechnology Advances* **33**(6):888–901 DOI [10.1016/j.biotechadv.2015.04.009](https://doi.org/10.1016/j.biotechadv.2015.04.009).
- Arnold K, Bordoli L, Kopp J, Schwede T. 2006.** The SWISS-MODEL workspace: a web-based environment for protein structure homology modelling. *Bioinformatics* **22**(2):195–201 DOI [10.1093/bioinformatics/bti770](https://doi.org/10.1093/bioinformatics/bti770).
- Aryal P, Sansom MSP, Tucker SJ. 2015.** Hydrophobic gating in ion channels. *Journal of Molecular Biology* **427**(1):121–130 DOI [10.1016/j.jmb.2014.07.030](https://doi.org/10.1016/j.jmb.2014.07.030).
- Bagal SK, Brown AD, Cox PJ, Omoto K, Owen RM, Pryde DC, Sidders B, Skerratt SE, Stevens EB, Storer RI, Swain NA. 2013.** Ion channels as therapeutic targets: a drug discovery perspective. *Journal of Medicinal Chemistry* **56**(3):593–624 DOI [10.1021/jm3011433](https://doi.org/10.1021/jm3011433).
- Benkert P, Tosatto SCE, Schomburg D. 2008.** QMEAN: a comprehensive scoring function for model quality assessment. *Proteins: Structure, Function, and Bioinformatics* **71**(1):261–277 DOI [10.1002/prot.21715](https://doi.org/10.1002/prot.21715).
- Berman H, Henrick K, Nakamura H, Markley JL. 2007.** The worldwide Protein Data Bank (wwPDB): ensuring a single, uniform archive of PDB data. *Nucleic Acids Research* **35**(Database):D301–D303 DOI [10.1093/nar/gkl971](https://doi.org/10.1093/nar/gkl971).
- Bernal RM, Tovar R, Santos JI, Munoz ML. 1998.** Possible role of calmodulin in excystation of *Giardia lamblia*. *Parasitology Research* **84**(9):687–693 DOI [10.1007/s004360050471](https://doi.org/10.1007/s004360050471).
- Bhattacharya D, Cheng J. 2013.** 3Drefine: consistent protein structure refinement by optimizing hydrogen bonding network and atomic-level energy minimization. *Proteins: Structure, Function, and Bioinformatics* **81**(1):119–131 DOI [10.1002/prot.24167](https://doi.org/10.1002/prot.24167).
- Bhattacharya D, Nowotny J, Cao R, Cheng J. 2016.** 3Drefine: an interactive web server for efficient protein structure refinement. *Nucleic Acids Research* **44**W1:W406–W409 DOI [10.1093/nar/gkw336](https://doi.org/10.1093/nar/gkw336).
- Biagini GA, Lloyd D, Kirk K, Edwards MR. 2000.** The membrane potential of *Giardia intestinalis*. *FEMS Microbiology Letters* **192**(1):153–157 DOI [10.1111/j.1574-6968.2000.tb09374.x](https://doi.org/10.1111/j.1574-6968.2000.tb09374.x).

- Biasini M, Bienert S, Waterhouse A, Arnold K, Studer G, Schmidt T, Kiefer F, Cassarino TG, Bertoni M, Bordoli L, Schwede T. 2014.** SWISS-MODEL: modelling protein tertiary and quaternary structure using evolutionary information. *Nucleic Acids Research* **42**(W1):W252–W258 DOI [10.1093/nar/gku340](https://doi.org/10.1093/nar/gku340).
- Bordoli L, Kiefer F, Arnold K, Benkert P, Battey J, Schwede T. 2008.** Protein structure homology modeling using SWISS-MODEL workspace. *Nature Protocols* **4**(1):1–13 DOI [10.1038/nprot.2008.197](https://doi.org/10.1038/nprot.2008.197).
- Bowie J, Luthy R, Eisenberg D. 1991.** A method to identify protein sequences that fold into a known three-dimensional structure. *Science* **253**(5016):164–170 DOI [10.1126/science.1853201](https://doi.org/10.1126/science.1853201).
- Calcada EO, Korsak M, Kozyreva T. 2015.** Recombinant intrinsically disordered proteins for NMR: tips and tricks. *Advances in Experimental Medicine and Biology* **870**:187–213 DOI [10.1007/978-3-319-20164-1_6](https://doi.org/10.1007/978-3-319-20164-1_6).
- Carter ER, Nabarro LE, Hedley L, Chiodini PL. 2018.** Nitroimidazole-refractory giardiasis: a growing problem requiring rational solutions. *Clinical Microbiology and Infection* **24**(1):37–42 DOI [10.1016/j.cmi.2017.05.028](https://doi.org/10.1016/j.cmi.2017.05.028).
- Chen YP, Chen F. 2008.** Identifying targets for drug discovery using bioinformatics. *Expert Opinion on Therapeutic Targets* **12**(4):383–389 DOI [10.1517/14728222.12.4.383](https://doi.org/10.1517/14728222.12.4.383).
- Cheng Y, LeGall T, Oldfield CJ, Mueller JP, Van YY, Romero P, Cortese MS, Uversky VN, Dunker AK. 2006.** Rational drug design via intrinsically disordered protein. *Trends in Biotechnology* **24**(10):435–442 DOI [10.1016/j.tibtech.2006.07.005](https://doi.org/10.1016/j.tibtech.2006.07.005).
- China G, Padron G, Hooft RWW, Sander C, Vriend G. 1995.** The use of position-specific rotamers in model building by homology. *Proteins: Structure, Function, and Bioinformatics* **23**(3):415–421 DOI [10.1002/prot.340230315](https://doi.org/10.1002/prot.340230315).
- Colovos C, Yeates TO. 1993.** Verification of protein structures: patterns of nonbonded atomic interactions. *Protein Science* **2**(9):1511–1519 DOI [10.1002/pro.5560020916](https://doi.org/10.1002/pro.5560020916).
- Conklin KA, Heu P, Chou SC. 1970.** Quinine-effect on *Tetrahymena pyriformis* 11: comparative activity of the stereoisomers, quinidine and quinine. *Journal of Pharmaceutical Sciences* **59**(5):704–705 DOI [10.1002/jps.2600590528](https://doi.org/10.1002/jps.2600590528).
- Corpet F. 1988.** Multiple sequence alignment with hierarchical clustering. *Nucleic Acids Research* **16**(22):10881–10890 DOI [10.1093/nar/16.22.10881](https://doi.org/10.1093/nar/16.22.10881).
- Dalton JA, Jackson RM. 2007.** An evaluation of automated homology modelling methods at low target template sequence similarity. *Bioinformatics* **23**(15):1901–1908 DOI [10.1093/bioinformatics/btm262](https://doi.org/10.1093/bioinformatics/btm262).
- Della Casa V, Noll H, Gonser S, Grob P, Graf F, Pohlig G. 2002.** Antimicrobial activity of dequalinium chloride against leading germs of vaginal infections. *Arzneimittelforschung* **52**(9):699–705 DOI [10.1055/s-0031-1299954](https://doi.org/10.1055/s-0031-1299954).
- Ellekvist P, Ricke CH, Litman T, Salanti A, Colding H, Zeuthen T, Klaerke DA. 2004.** Molecular cloning of a K(+) channel from the malaria parasite *Plasmodium falciparum*. *Biochemical and Biophysical Research Communications* **318**(2):477–484 DOI [10.1016/j.bbrc.2004.04.049](https://doi.org/10.1016/j.bbrc.2004.04.049).
- Escobedo AA, Cimerman S. 2007.** Giardiasis: a pharmacotherapy review. *Expert Opinion on Pharmacotherapy* **8**(12):1885–1902 DOI [10.1517/14656566.8.12.1885](https://doi.org/10.1517/14656566.8.12.1885).
- Ferreira LG, Dos Santos RN, Oliva G, Andricopulo AD. 2015.** Molecular docking and structure-based drug design strategies. *Molecules* **20**(7):13384–13421 DOI [10.3390/molecules200713384](https://doi.org/10.3390/molecules200713384).
- Fiser A, Do RK, Sali A. 2000.** Modeling of loops in protein structures. *Protein Science* **9**(9):1753–1773 DOI [10.1110/ps.9.9.1753](https://doi.org/10.1110/ps.9.9.1753).

- Grunnet M, MacAulay N, Jorgensen NK, Jensen B, Olesen S-P, Klaerke DA. 2002. Regulation of cloned, Ca²⁺-activated K⁺ channels by cell volume changes. *Pflügers Archiv* **444**(1–2):167–177 DOI [10.1007/s00424-002-0782-4](https://doi.org/10.1007/s00424-002-0782-4).
- Henikoff S, Henikoff JG. 1994. Protein family classification based on searching a database of blocks. *Genomics* **19**(1):97–107 DOI [10.1006/geno.1994.1018](https://doi.org/10.1006/geno.1994.1018).
- Irwin JJ, Sterling T, Mysinger MM, Bolstad ES, Coleman RG. 2012. ZINC: a free tool to discover chemistry for biology. *Journal of Chemical Information and Modeling* **52**(7):1757–1768 DOI [10.1021/ci3001277](https://doi.org/10.1021/ci3001277).
- Jimenez V, Docampo R. 2012. Molecular and electrophysiological characterization of a novel cation channel of *Trypanosoma cruzi*. *PLOS Pathogens* **8**(6):e1002750 DOI [10.1371/journal.ppat.1002750](https://doi.org/10.1371/journal.ppat.1002750).
- Jones P, Binns D, Chang HY, Fraser M, Li W, McAnulla C, McWilliam H, Maslen J, Mitchell A, Nuka G, Pesseat S, Quinn AF, Sangrador-Vegas A, Scheremetjew M, Yong SY, Lopez R, Hunter S. 2014. InterProScan 5: genome-scale protein function classification. *Bioinformatics* **30**(9):1236–1240 DOI [10.1093/bioinformatics/btu031](https://doi.org/10.1093/bioinformatics/btu031).
- Kelley LA, Mezulis S, Yates CM, Wass MN, Sternberg MJE. 2015. The Phyre2 web portal for protein modeling, prediction and analysis. *Nature Protocols* **10**(6):845–858 DOI [10.1038/nprot.2015.053](https://doi.org/10.1038/nprot.2015.053).
- Kingsley B, Kumari S, Appian S, Brindha P. 2017. In silico docking studies on ATP-sensitive K⁺Channel, insulin receptor and phosphorylase kinase activity by isolated active principles of *stereospermum tetragonum* DC. *Journal of Young Pharmacists* **9**(1):124–126 DOI [10.5530/jyp.2017.9.23](https://doi.org/10.5530/jyp.2017.9.23).
- Kufareva I, Abagyan R. 2012. Methods of protein structure comparison. *Methods in Molecular Biology* **857**:231–257 DOI [10.1007/978-1-61779-588-6_10](https://doi.org/10.1007/978-1-61779-588-6_10).
- Leitsch D. 2015. Drug resistance in the microaerophilic parasite *Giardia lamblia*. *Current Tropical Medicine Reports* **2**(3):128–135 DOI [10.1007/s40475-015-0051-1](https://doi.org/10.1007/s40475-015-0051-1).
- Liu K, Kokubo H. 2017. Exploring the stability of ligand binding modes to proteins by molecular dynamics simulations: a cross-docking study. *Journal of Chemical Information and Modeling* **57**(10):2514–2522 DOI [10.1021/acs.jcim.7b00412](https://doi.org/10.1021/acs.jcim.7b00412).
- Liu H, Li Y, Song M, Tan X, Cheng F, Zheng S, Shen J, Luo X, Ji R, Yue J, Hu G, Jiang H, Chen K. 2003. Structure-based discovery of potassium channel blockers from natural products: virtual screening and electrophysiological assay testing. *Chemistry & Biology* **10**(11):1103–1113 DOI [10.1016/j.chembiol.2003.10.011](https://doi.org/10.1016/j.chembiol.2003.10.011).
- Lovell SC, Davis IW, Arendall WB, De Bakker PIW, Word JM, Prisant MG, Richardson JS, Richardson DC. 2003. Structure validation by C α geometry: ϕ , ψ and C β deviation. *Proteins: Structure, Function, and Bioinformatics* **50**(3):437–450 DOI [10.1002/prot.10286](https://doi.org/10.1002/prot.10286).
- Luthy R, Bowie JU, Eisenberg D. 1992. Assessment of protein models with three-dimensional profiles. *Nature* **356**(6364):83–85 DOI [10.1038/356083a0](https://doi.org/10.1038/356083a0).
- Ma J, Peng J, Wang S, Xu J. 2012. A conditional neural fields model for protein threading. *Bioinformatics* **28**(12):i59–i66 DOI [10.1093/bioinformatics/bts213](https://doi.org/10.1093/bioinformatics/bts213).
- Ma J, Wang S, Zhao F, Xu J. 2013. Protein threading using context-specific alignment potential. *Bioinformatics* **29**(13):i257–i265 DOI [10.1093/bioinformatics/btt210](https://doi.org/10.1093/bioinformatics/btt210).
- Marchler-Bauer A, Bo Y, Han L, He J, Lanczycki CJ, Lu S, Chitsaz F, Derbyshire MK, Geer RC, Gonzales NR, Gwadz M, Hurwitz DI, Lu F, Marchler GH, Song JS, Thanki N, Wang Z, Yamashita RA, Zhang D, Zheng C, Geer LY, Bryant SH. 2017. CDD/SPARCLE: functional classification of proteins via subfamily domain architectures. *Nucleic Acids Research* **45**(D1):D200–D203 DOI [10.1093/nar/gkw1129](https://doi.org/10.1093/nar/gkw1129).

- Maroulis SL, Schofield PJ, Edwards MR. 2000.** The role of potassium in the response of *Giardia intestinalis* to hypo-osmotic stress. *Molecular and Biochemical Parasitology* **108**(1):141–145 DOI [10.1016/s0166-6851\(00\)00203-6](https://doi.org/10.1016/s0166-6851(00)00203-6).
- Martí-Renom MA, Stuart AC, Fiser A, Sánchez R, Melo F, Šali A. 2000.** Comparative protein structure modeling of genes and genomes. *Annual Review of Biophysics and Biomolecular Structure* **29**(1):291–325 DOI [10.1146/annurev.biophys.29.1.291](https://doi.org/10.1146/annurev.biophys.29.1.291).
- Martins LC, Torres PHM, De Oliveira RB, Pascutti PG, Cino EA, Ferreira RS. 2018.** Investigation of the binding mode of a novel cruzain inhibitor by docking, molecular dynamics, ab initio and MM/PBSA calculations. *Journal of Computer-Aided Molecular Design* **32**(5):591–605 DOI [10.1007/s10822-018-0112-3](https://doi.org/10.1007/s10822-018-0112-3).
- Marzian S, Stansfeld PJ, Rapedius M, Rinne S, Nematian-Ardestani E, Abbruzzese JL, Steinmeyer K, Sansom MSP, Sanguinetti MC, Baukowitz T, Decher N. 2013.** Side pockets provide the basis for a new mechanism of Kv channel-specific inhibition. *Nature Chemical Biology* **9**(8):507–513 DOI [10.1038/nchembio.1271](https://doi.org/10.1038/nchembio.1271).
- Nam TG, McNamara CW, Bopp S, Dharia NV, Meister S, Bonamy GM, Plouffe DM, Kato N, McCormack S, Bursulaya B, Ke H, Vaidya AB, Schultz PG, Winzeler EA. 2011.** A chemical genomic analysis of decoquinate, a *Plasmodium falciparum* cytochrome b inhibitor. *ACS Chemical Biology* **6**(11):1214–1222 DOI [10.1021/cb200105d](https://doi.org/10.1021/cb200105d).
- Obradovic Z, Peng K, Vucetic S, Radivojac P, Brown CJ, Dunker AK. 2003.** Predicting intrinsic disorder from amino acid sequence. *Proteins: Structure, Function, and Genetics* **53**(S6):566–572 DOI [10.1002/prot.10532](https://doi.org/10.1002/prot.10532).
- Otter T, Satir BH, Satir P. 1984.** Trifluoperazine-induced changes in swimming behavior of paramecium: evidence for two sites of drug action. *Cell Motility* **4**(4):249–267 DOI [10.1002/cm.970040404](https://doi.org/10.1002/cm.970040404).
- Pchelintseva E, Djamgoz MBA. 2018.** Mesenchymal stem cell differentiation: Control by calcium-activated potassium channels. *Journal of Cellular Physiology* **233**(5):3755–3768 DOI [10.1002/jcp.26120](https://doi.org/10.1002/jcp.26120).
- Peng J, Xu J. 2010.** Low-homology protein threading. *Bioinformatics* **26**(12):i294–i300 DOI [10.1093/bioinformatics/btq192](https://doi.org/10.1093/bioinformatics/btq192).
- Pettersen EF, Goddard TD, Huang CC, Couch GS, Greenblatt DM, Meng EC, Ferrin TE. 2004.** UCSF Chimera—a visualization system for exploratory research and analysis. *Journal of Computational Chemistry* **25**(13):1605–1612 DOI [10.1002/jcc.20084](https://doi.org/10.1002/jcc.20084).
- Ponce A, Jimenez-Cardoso E, Eligio-Garcia L. 2013.** Voltage-dependent potassium currents expressed in *Xenopus laevis* oocytes after injection of mRNA isolated from trophozoites of *Giardia lamblia* (strain Portland-1). *Physiological Reports* **1**(7):e00186 DOI [10.1002/phy2.186](https://doi.org/10.1002/phy2.186).
- Prole DL, Marrion NV. 2012.** Identification of putative potassium channel homologues in pathogenic protozoa. *PLOS ONE* **7**(2):e32264 DOI [10.1371/journal.pone.0032264](https://doi.org/10.1371/journal.pone.0032264).
- Rateb ME, Hallyburton I, Houssen WE, Bull AT, Goodfellow M, Santhanam R, Jaspars M, Ebel R. 2013.** Induction of diverse secondary metabolites in *Aspergillus fumigatus* by microbial co-culture. *RSC Advances* **3**(34):14444 DOI [10.1039/c3ra42378f](https://doi.org/10.1039/c3ra42378f).
- Rezaei F, Ebrahimzadeh MA, Daryani A, Sharif M, Ahmadpour E, Sarvi S. 2016.** The inhibitory effect of cromolyn sodium and ketotifen on *Toxoplasma gondii* entrance into host cells in vitro and in vivo. *Journal of Parasitic Diseases* **40**(3):1001–1005 DOI [10.1007/s12639-014-0623-3](https://doi.org/10.1007/s12639-014-0623-3).
- Roy A, Kucukural A, Zhang Y. 2010.** I-TASSER: a unified platform for automated protein structure and function prediction. *Nature Protocols* **5**(4):725–738 DOI [10.1038/nprot.2010.5](https://doi.org/10.1038/nprot.2010.5).

- Šali A, Blundell TL. 1993. Comparative protein modelling by satisfaction of spatial restraints. *Journal of Molecular Biology* 234(3):779–815 DOI 10.1006/jmbi.1993.1626.
- Saxena P, Zangerl-Plessl EM, Linder T, Windisch A, Hohaus A, Timin E, Hering S, Stary-Weinzinger A. 2016. New potential binding determinant for hERG channel inhibitors. *Scientific Reports* 6(1):24182 DOI 10.1038/srep24182.
- Schmidt RS, Macedo JP, Steinmann ME, Salgado AG, Butikofer P, Sigel E, Rentsch D, Maser P. 2018. Transporters of Trypanosoma brucei-phylogeny, physiology, pharmacology. *FEBS Journal* 285(6):1012–1023 DOI 10.1111/febs.14302.
- Schwab A, Hanley P, Fabian A, Stock C. 2008. Potassium channels keep mobile cells on the go. *Physiology* 23(4):212–220 DOI 10.1152/physiol.00003.2008.
- Shin N, Soh H, Chang S, Kim DH, Park CS. 2005. Sodium permeability of a cloned small-conductance calcium-activated potassium channel. *Biophysical Journal* 89(5):3111–3119 DOI 10.1529/biophysj.105.069542.
- Sigrist CJ, De Castro E, Cerutti L, Cuche BA, Hulo N, Bridge A, Bougueleret L, Xenarios I. 2013. New and continuing developments at PROSITE. *Nucleic Acids Research* 41(D1):D344–D347 DOI 10.1093/nar/gks1067.
- Singh N, Puri SK. 1998. Causal prophylactic activity of antihistaminic agents against Plasmodium yoelii nigeriensis infection in Swiss mice. *Acta Tropica* 69(3):255–260 DOI 10.1016/s0001-706x(97)00138-1.
- Steinmann ME, Gonzalez-Salgado A, Butikofer P, Maser P, Sigel E. 2015. A heteromeric potassium channel involved in the modulation of the plasma membrane potential is essential for the survival of African trypanosomes. *FASEB Journal* 29(8):3228–3237 DOI 10.1096/fj.15-271353.
- Studer G, Biasini M, Schwede T. 2014. Assessing the local structural quality of transmembrane protein models using statistical potentials (QMEANBrane). *Bioinformatics* 30(17):i505–i511 DOI 10.1093/bioinformatics/btu457.
- Subramanyam P, Colecraft HM. 2015. Ion channel engineering: perspectives and strategies. *Journal of Molecular Biology* 427(1):190–204 DOI 10.1016/j.jmb.2014.09.001.
- Tejman-Yarden N, Eckmann L. 2011. New approaches to the treatment of giardiasis. *Current Opinion in Infectious Diseases* 24(5):451–456 DOI 10.1097/QCO.0b013e32834ad401.
- Trott O, Olson AJ. 2010. AutoDock Vina: improving the speed and accuracy of docking with a new scoring function, efficient optimization, and multithreading. *Journal of Computational Chemistry* 31(2):455–461 DOI 10.1002/jcc.21334.
- Tusnady GE, Simon I. 1998. Principles governing amino acid composition of integral membrane proteins: application to topology prediction. *Journal of Molecular Biology* 283(2):489–506 DOI 10.1006/jmbi.1998.2107.
- Tusnady GE, Simon I. 2001. The HMMTOP transmembrane topology prediction server. *Bioinformatics* 17(9):849–850 DOI 10.1093/bioinformatics/17.9.849.
- Urrego D, Tomczak AP, Zahed F, Stuhmer W, Pardo LA. 2014. Potassium channels in cell cycle and cell proliferation. *Philosophical Transactions of the Royal Society B: Biological Sciences* 369(1638):20130094 DOI 10.1098/rstb.2013.0094.
- Waller KL, McBride SM, Kim K, McDonald TV. 2008. Characterization of two putative potassium channels in Plasmodium falciparum. *Malaria Journal* 7(1):19 DOI 10.1186/1475-2875-7-19.
- Watkins RR, Eckmann L. 2014. Treatment of giardiasis: current status and future directions. *Current Infectious Disease Reports* 16(2):396 DOI 10.1007/s11908-014-0396-y.

- Webb B, Sali A. 2014.** Comparative Protein Structure Modeling Using MODELLER. *Current Protocols in Bioinformatics* 47:5.6.1–5.6.32 DOI [10.1002/0471250953.bi0506s47](https://doi.org/10.1002/0471250953.bi0506s47).
- Wiederstein M, Sippl MJ. 2007.** ProSA-web: interactive web service for the recognition of errors in three-dimensional structures of proteins. *Nucleic Acids Research* 35(Web Server):W407–W410 DOI [10.1093/nar/gkm290](https://doi.org/10.1093/nar/gkm290).
- Wilkins MR, Gasteiger E, Bairoch A, Sanchez JC, Williams KL, Appel RD, Hochstrasser DF. 1999.** Protein identification and analysis tools in the ExPASy server. *2-D Proteome Analysis Protocols* 112:531–552 DOI [10.1385/1-59259-584-7:531](https://doi.org/10.1385/1-59259-584-7:531).
- Wulff H, Castle NA, Pardo LA. 2009.** Voltage-gated potassium channels as therapeutic targets. *Nature Reviews Drug Discovery* 8(12):982–1001 DOI [10.1038/nrd2983](https://doi.org/10.1038/nrd2983).
- Yachdav G, Kloppmann E, Kajan L, Hecht M, Goldberg T, Hamp T, Honigschmid P, Schafferhans A, Roos M, Bernhofer M, Richter L, Ashkenazy H, Punta M, Schlessinger A, Bromberg Y, Schneider R, Vriend G, Sander C, Ben-Tal N, Rost B. 2014.** PredictProtein—an open resource for online prediction of protein structural and functional features. *Nucleic Acids Research* 42(W1):W337–W343 DOI [10.1093/nar/gku366](https://doi.org/10.1093/nar/gku366).
- Yang J, Yan R, Roy A, Xu D, Poisson J, Zhang Y. 2015.** The I-TASSER Suite: protein structure and function prediction. *Nature Methods* 12(1):7–8 DOI [10.1038/nmeth.3213](https://doi.org/10.1038/nmeth.3213).
- Zhang Y. 2008.** I-TASSER server for protein 3D structure prediction. *BMC Bioinformatics* 9(1):40 DOI [10.1186/1471-2105-9-40](https://doi.org/10.1186/1471-2105-9-40).